

Journal of Visualized Experiments

Monovalent Cation Doping of CH₃NH₃PbI₃ for Efficient Perovskite Solar Cells

--Manuscript Draft--

Manuscript Number:	JoVE55307R2
Full Title:	Monovalent Cation Doping of CH ₃ NH ₃ PbI ₃ for Efficient Perovskite Solar Cells
Article Type:	Invited Methods Article - JoVE Produced Video
Keywords:	Monovalent cation halide; additives; CH ₃ NH ₃ PbI ₃ Perovskite; doping; surface passivation
Manuscript Classifications:	92.23: Chemistry and Materials (General); 92.25: Inorganic, Organic and Physical Chemistry; 93.33: Electronics and Electrical Engineering; 97.70: Physics (General)
Corresponding Author:	Mojtaba Abdi-Jalebi University of Cambridge Cambridge , Cambridgeshire UNITED KINGDOM
Corresponding Author Secondary Information:	
Corresponding Author E-Mail:	ma571@cam.ac.uk
Corresponding Author's Institution:	University of Cambridge
Corresponding Author's Secondary Institution:	
First Author:	Mojtaba Abdi-Jalebi
First Author Secondary Information:	
Other Authors:	Mohammad Ibrahim Dar
	Aditya Sadhanala
	Satyaprasad P. Senanayak
	Michael Grätzel
	Richard H. Friend
Order of Authors Secondary Information:	
Abstract:	We demonstrate the incorporation of monovalent cation additives into CH ₃ NH ₃ PbI ₃ perovskite in order to tune the optical, excitonic and electrical properties. The possibility of doping is investigated by adding monovalent cation halide with similar ionic radii to Pb ²⁺ , including Cu ⁺ , Na ⁺ and Ag ⁺ where a shift in the Fermi level and a remarkable decrease of subbandgap optical absorption along with lower energetic disorder of the perovskite is achieved. An order of magnitude enhancement in the bulk hole mobility and a significant reduction of transport activation energy within additive-based perovskite device is attained. The confluence of aforementioned improved properties in the presence of these cations lead to an enhancement in the photovoltaic parameters of the perovskite solar cell. An increase of 70 mV in open circuit voltage for AgI and a 2 mA.cm ⁻² improvement in photocurrent density for NaI and CuBr based solar cells are achieved compare to the pristine device. Our work paves the way for further improvement of the optoelectronic quality of CH ₃ NH ₃ PbI ₃ perovskite, and subsequent devices, via highlighting a new avenue for investigation of the role of dopant impurities upon crystallisation and controlling the electronic defect density in the perovskite structures.
Author Comments:	We have inserted the figures in TIF format. Since we have exported them from ppt, the quality of the images is not high. We can provide the ppt of the figures and table upon request. The .xls format of the tables are provided.
Additional Information:	

Question	Response
If this article needs to be "in-press" by a certain date, please indicate the date below and explain in your cover letter.	

TITLE:**Monovalent Cation Doping of $\text{CH}_3\text{NH}_3\text{PbI}_3$ for Efficient Perovskite Solar Cells****AUTHORS:**

Mojtaba Abdi-Jalebi
Cavendish Laboratory
University of Cambridge
Cambridge, UK
ma571@cam.ac.uk

M. Ibrahim Dar
Institute of Chemical Sciences and Engineering
École Polytechnique Fédérale de Lausanne
Lausanne, Switzerland
Ibrahim.dar@epfl.ch

Aditya Sadhanala
Cavendish Laboratory
University of Cambridge
Cambridge, UK
as2233@cam.ac.uk

Satyaprasad P. Senanayak
Cavendish Laboratory
University of Cambridge
Cambridge, UK
sps54@cam.ac.uk

Michael Grätzel
Institute of Chemical Sciences and Engineering
École Polytechnique Fédérale de Lausanne
Lausanne, Switzerland
michael.graetzel@epfl.ch

Richard H. Friend
Cavendish Laboratory
University of Cambridge
Cambridge, UK
rhf10@cam.ac.uk

CORRESPONDING AUTHOR:

Mojtaba Abdi-Jalebi (ma571@cam.ac.uk)

KEYWORDS:

Monovalent cation halide; additives; $\text{CH}_3\text{NH}_3\text{PbI}_3$ perovskite; doping; surface passivation

SHORT ABSTRACT:

Here, we present a protocol to adjust the properties of solution-processed $\text{CH}_3\text{NH}_3\text{PbI}_3$ through the incorporation of monovalent cation additives in order to achieve highly efficient perovskite solar cells.

LONG ABSTRACT:

Here, we demonstrate the incorporation of monovalent cation additives into $\text{CH}_3\text{NH}_3\text{PbI}_3$ perovskite in order to adjust the optical, excitonic, and electrical properties. The possibility of doping was investigated by adding monovalent cation halides with similar ionic radii to Pb^{2+} , including Cu^+ , Na^+ , and Ag^+ . A shift in the Fermi level and a remarkable decrease of sub-bandgap optical absorption, along with a lower energetic disorder in the perovskite, was achieved. An order-of-magnitude enhancement in the bulk hole mobility and a significant reduction of transport activation energy within an additive-based perovskite device was attained. The confluence of the aforementioned improved properties in the presence of these cations led to an enhancement in the photovoltaic parameters of the perovskite solar cell. An increase of 70 mV in open circuit voltage for AgI and a 2-mA/cm² improvement in photocurrent density for NaI- and CuBr-based solar cells were achieved compared to the pristine device. Our work paves the way for further improvements in the optoelectronic quality of $\text{CH}_3\text{NH}_3\text{PbI}_3$ perovskite and subsequent devices. It highlights a new avenue for investigations on the role of dopant impurities in crystallization and controls the electronic defect density in perovskite structures.

INTRODUCTION:

Currently, the dominant portion of the world's energy requirement (*i.e.*, 85%) is being supplied by the combustion of oil, coal, and natural gas, which facilitates global warming and has deleterious effects on our environment¹. Therefore, the development of CO₂-neutral sources of energy is of paramount interest. Photovoltaics (PV) is an ideal energy conversion process that can meet this requirement. However, cost and efficiency, as the main obstacles to the extensive adoption of PV technology, must be improved. Emerging PV technologies based on new materials, such as perovskite solar cells (PSC), have the combination of lower cost and greater efficiency. This is achieved through the utilization of cheap materials that are readily available, as well as through fast, facile, and low-energy processing routes compared to silicon-based counterparts²⁻⁴. A remarkable improvement in the power conversion efficiency (PCE), from 3.8% to more than 22%, has been reported for hybrid organic-inorganic lead halide perovskite since its first appearance in PV architecture⁵⁻⁸. Such a superb performance originates from the strong light absorption with an extremely sharp band-edge, the very low energetic disorder, the weakly-bound excitons that easily dissociate into free carriers with large diffusion lengths, and the photon recycling capability of hybrid organic-inorganic lead halide perovskite⁹⁻¹². These materials are categorized in the perovskite family, which are crystallized from organic halide and metal halide salts to form crystals in the ABX_3 structure, where X is an anion and A and B are cations of different sizes (A being larger than B). Reported cations for the A site include methylammonium (MA), formamidinium (FA), and cesium (Cs); a combination of these cations shows the highest performance^{13,14}. Furthermore, the main candidate for the divalent cation in

the B site is lead, which can be replaced by tin; the bandgap can be successfully red-shifted to over 1,000 nm in a lead-tin mixed perovskite¹⁵. Similarly, the X-site occupants have been studied extensively, where a mixture of iodide (I) and bromide (Br) were introduced as the main candidates^{16,17}. Therefore, it is highly plausible to manipulate the structural, morphological, and optoelectronic properties of perovskites by altering their chemical composition.

Despite the fact that the enhanced crystalline quality and the macroscopic uniformity of the perovskite film are key parameters to achieve efficient devices¹⁸, the impact of the boundaries between the polycrystalline domains, the origin and role of electronic defects in the perovskite absorbers, and the role of the charge collection layers upon loss processes in the perovskite solar cells are not yet well understood. Regarding the nature of electronic defects in the perovskite structure, it has been reported that many of the defects, such as I or Pb vacancies, result in states that are very close to or within the continuum of states in the conduction and valence bands, which might have a negative electronic impact on the photovoltaic devices¹⁹. In addition, a strong covalent bonding interaction between lead cations and iodide anions in the perovskite plane may lead to the existence of intrinsic defects (*e.g.*, under-coordinated Pb dimers and I trimers), which could create sites within the band-edge that act as charge recombination centers during the operation of the device²⁰.

Here, we investigate the impact of doping $\text{CH}_3\text{NH}_3\text{PbI}_3$ perovskite with monovalent cation halides, including Na^+ , Cu^+ , and Ag^+ , lower-valence metal ions than Pb^{2+} . We therefore incorporate these cations through the addition of a rational amount of their halide-based salts (*e.g.*, NaI, CuBr, CuI, and AgI) into the perovskite precursor solution. These cations have ionic radii similar to Pb^{2+} , so substitutional doping within the crystal is probable. We have shown that the presence of these cations strongly affects both the morphology and coverage of the perovskite layer. In addition, the presence of these cations (*e.g.*, Na^+ and Ag^+) has been confirmed by X-ray photoelectron spectroscopy (XPS), and a significant change in the Fermi level of perovskite was measured by Kelvin probe force microscopy (KPFM). By incorporating these cations into sequentially deposited perovskite solar cells, we achieved an improvement in the photovoltaic efficiency of PSC (15.6% compare to 14%). Therefore, it is very essential to enhance the structural and optoelectronic properties of the absorber layer (*e.g.*, perovskite) in solar cell architecture to maximize the charge transport and to passivate the surface traps in order to reach the highest PV performance.

PROTOCOL:

1. Synthesis and deposition of pristine and additive-based $\text{CH}_3\text{NH}_3\text{PbI}_3$

Note: All the solutions were prepared inside an argon glove box under moisture- and oxygen-controlled conditions (H_2O level: <1 ppm and O_2 level: <10 ppm).

1.1) Dissolve 553 mg (1.2 M) of PbI_2 in 1 mL of N,N-dimethylformamide (DMF) under constant stirring at 80 °C.

1.2) Add 0.02 M of monovalent cation halides to the PbI_2 solution.

- 1.3) Spin-coat the resulting yellow transparent solution onto the substrate (*e.g.*, mesoporous-TiO₂) for 30 s at 6,500 rpm with a ramp of 4,000 rpm.
- 1.4) Bake the films on a hotplate at 80 °C for 30 min.
- 1.5) Dissolve 40 mg of methylammonium iodide (MAI) in 5 mL of isopropanol.
- 1.6) Spin-coat a sufficient amount of MAI solution onto the resulting lead iodide films using a two-step protocol that includes 45 s of loading time followed by 20 s of spinning at 4,000 rpm.
- 1.7) Anneal the spin-coated perovskite films on a hotplate at 100 °C for 45 min.

2. Solar cell fabrication

2.1) Substrate preparation

- 2.1.1) Pattern fluorine-doped tin oxide (FTO)-coated glass.
 - 2.1.1.1) Cover the active area of the FTO glass with semitransparent adhesive tape.
 - 2.1.1.2) Pour the zinc (Zn) powder on the uncovered areas of the FTO substrates.
 - 2.1.1.3) Prepare 2 M of hydrochloric acid (HCl) in distilled water.
 - 2.1.1.4) Pour the HCl solution onto the part of the FTO glass that is covered with Zn powder.
 - 2.1.1.5) Wash the FTO with water and remove the tape.
- 2.1.2) **Cleaning the substrates**
 - 2.1.2.1) Wash the FTO glass using 2% (w/v) detergent.
 - 2.1.2.2) Sonicate the etched FTO substrates in acetone and isopropanol (IPA) for 10 min.
 - 2.1.2.3) Treat the FTO substrates with an ultraviolet/O₃ cleaner for 15 min.

2.2) Deposition of a hole blocking layer

- 2.2.1) Add 0.6 mL of titanium diisopropoxide bis(acetylacetonate) (TAA) in 7 mL of IPA.
- 2.2.2) Put the cleaned and patterned FTO substrates on a hotplate at 450 °C and cover the contact area before heating.
- 2.2.3) Spray pyrolysis the TAA solution onto the uncovered area using O₂ as the carrier gas.

2.2.4) Leave the samples at 450 °C for 30 min.

2.3) **Deposition of an electron transport layer**

2.3.1) Dilute the commercial TiO₂ paste (30-nm particle size) with ethanol (2:7, weight ratio).

2.3.2) Homogenize the TiO₂ dilution by sonicating for 30 min.

2.3.3) Spin-coat the titania dilution onto the prepared samples with compact TiO₂ layers for 30 s at 5,000 rpm with a ramp of 2,000 rpm.

2.3.4) Anneal the titania films at 500 °C for 30 min.

2.3.5) Treat the resulting mesoporous TiO₂ films in a 40-mM solution of TiCl₄ in distilled water for 20 min.

2.3.6) Anneal the TiCl₄-treated films at 450 °C for 30 min.

2.4) **Deposition of the perovskite layer**

Note: The FTO substrates with titania layers were transferred to a dry-air box with a humidity of <1% for the rest of the fabrication process.

2.4.1) Spin-coat the prepared lead iodide solutions (with and without dopants) onto the mesoporous TiO₂ for 30 s at 6,500 rpm with a ramp of 4,000 rpm.

2.4.2) Bake the films on a hotplate at 80 °C for 30 min.

2.4.3) Spin-coat a sufficient amount of MAI solution into the resulting lead iodide films using a two-step protocol that includes 45 s of loading time followed by spinning for 20 s at 4,000 rpm with a ramp of 2,000 rpm.

2.4.4) Anneal the spin-coated perovskite films on a hotplate at 100 °C for 45 min.

2.5. **Deposition of the hole transport layer**

2.5.1) Add 72.3 mg of spiro-OMeTAD to 1 mL of chlorobenzene and shake until the solution becomes transparent.

2.5.2) Make a stock solution of bis(trifluoromethylsulfonyl)imide (LiTFSI) by adding 520 mg of LiTFSI in acetonitrile.

2.5.3) Add 17.5 µL of the LiTFSI stock solution and 28.8 µL of 4-tert-butylpyridine (TBP) to the spiro-OMeTAD solution.

2.5.4) Spin-coat the above solution for 30 s at 4,000 rpm with a ramp of 2,000 rpm.

2.6. Thermal evaporation of the top contact

2.6.1) Mask the samples and put them in the vacuum chamber of the evaporator.

2.6.2) Evaporate 80 nm of gold at a rate of 0.01 nm/s.

REPRESENTATIVE RESULTS:

Field emission scanning electron microscopy (FESEM) was used to record both cross-sectional images of the fabricated perovskite solar cells (Figure 1) and top view images of the deposited PbI_2 and $\text{CH}_3\text{NH}_3\text{PbI}_3$ films (Figure 2). X-ray diffraction (XRD) and X-ray photoelectron spectroscopy (XPS) were employed to characterize the structural properties of the perovskite films (Figures 3 and 4). Photothermal deflection spectroscopy (PDS) and Kelvin probe force microscopy (KPFM) were used to probe the optical and electrical properties of the perovskite films, respectively (Figures 5 and 6). Furthermore, temperature-dependent bulk transport measurements based on space charge limited current (SCLC) was performed on the perovskite devices (Figure 7). Finally, a standard photovoltaic measurement of the fabricated devices was performed (Figure 8 and Table 1).

Based on the top-view SEM images of the PbI_2 and $\text{CH}_3\text{NH}_3\text{PbI}_3$ deposited on the mesoporous TiO_2 layer (mp- TiO_2) shown in Figure 2, the effect of the additives on the morphology of perovskite was illustrated where large branch-shaped crystals of PbI_2 were achieved in the NaI-based sample. This led to the formation of larger asymmetric crystals of perovskite. Furthermore, we obtained a uniform and pinhole-free perovskite capping layer for CuI- and AgI-based samples (Figure 2c and e). To investigate the effect of monovalent cation halide additives on the crystal structure of $\text{CH}_3\text{NH}_3\text{PbI}_3$ and on the conversion of PbI_2 into $\text{CH}_3\text{NH}_3\text{PbI}_3$, X-ray diffraction was performed (Figure 3). Although the crystal structure of the final perovskite remained the same for all samples, it is evident that the diffraction peak at $2\theta = 12.6$, which corresponds to the unconverted PbI_2 , was eliminated in the presence of NaI and CuBr additives. In order to confirm the presence of these monovalent cations within the $\text{CH}_3\text{NH}_3\text{PbI}_3$ perovskite films, we carried out an XPS analysis, as shown in Figure 4. On the basis of the XPS data, we demonstrated the presence of Na and Ag ions within the perovskite films, whereas the concentration of Cu could not be estimated, probably due to the nearness of iodide (I 3p_{1/2}) and copper (Cu 2p_{1/2}) peaks.

The effect of the monovalent cation additives on the absorption spectrum of the perovskite is shown in Figure 5a, which was measured by PDS. It is evident that the additive-based $\text{CH}_3\text{NH}_3\text{PbI}_3$ had lower sub-bandgap absorption compared to the pristine sample. Furthermore, an absorption tail was observed for Cu-based samples, which originated from the intrinsic absorption of copper halide (Figure 5b). Although the absorption tail confirms the presence of Cu cations in the final perovskite films, it is evident, based on the comparison between the PDS of CuI-based PbI_2 and $\text{CH}_3\text{NH}_3\text{PbI}_3$, that their incorporation is not complete. In addition, the Urbach energy (E_u), which is a measure of the degree of energetic disorder of a material, was estimated for pristine, NaI-, CuBr-, CuI-, and AgI-based perovskite, and the values are 15.6, 11.8, 12.8, 13.5, and 15.2 meV,

respectively (inset of Figure 5a).

To explore the influence of the aforementioned additives on the electronic structure of $\text{CH}_3\text{NH}_3\text{PbI}_3$, we performed KPFM, where the contact potential difference (CPD) of the line profiles was measured. This corresponds to the surface work function (Φ) of the perovskite shown in Figure 6. A clear shift in the CPD (*i.e.*, 0.1 V) of additive-based perovskite compared to the pristine one shows that the perovskite Fermi level is shifted towards the valence band. This change in the Fermi level of perovskite can be attributed to either substitutional p-doping (*e.g.*, the replacement of Pb^{2+} with monovalent cations X^+) or surface passivation at the crystalline surfaces of perovskite.

To investigate the effect of doping on the density of the charges and on their transport properties in $\text{CH}_3\text{NH}_3\text{PbI}_3$, we performed temperature-dependent bulk transport measurements (Figure 7a). We then estimated the bulk carrier mobility (μ_{SCL}) based on the space charge limited current (SCLC) of the complete electron and hole-only pristine and additive-based perovskite devices. A remarkable increase in the conductivity and in both the electron and hole mobilities were achieved, particularly for the NaI and CuBr samples compared to pristine perovskite (Table 1). It is notable that the improvement in the charge mobility and conductivity are consistent with the enhancement in the short circuit current (J_{sc}) and fill factor (FF) of the fabricated solar cells shown in Figure 7b. Furthermore, we estimated the activation energy for charge transport (E_{A}) for both the electron and the hole using temperature-dependent bulk transport measurements, where a clear decrease was achieved for additive-based perovskite. This improvement is attributed to the higher density of carriers because of doping and filling the transport traps, which results in a significant decline in the transport barrier.

We fabricated perovskite solar cells based on the aforementioned monovalent cation halides, the corresponding J-V curves, and the photovoltaic parameters that are summarized in Figure 8a and Table 1. A significant improvement in open circuit voltage was achieved for both CuI- (0.99 V) and AgI- (1.02 V) based solar cells because of the ideal surface coverage (Figure 2c and e). Furthermore, a remarkable increase in the short circuit current ($\approx 2 \text{ mA cm}^{-2}$) for CuBr- and NaI-based solar cells was attained, which can be ascribed to the full conversion of PbI_2 into $\text{CH}_3\text{NH}_3\text{PbI}_3$. This improvement was confirmed by the incident photon-to-current conversion efficiency (IPCE) spectra shown in Figure 8b. Finally, higher power conversion efficiency (PCE) levels of 15.2%, 15.6%, and 15.3% were achieved for NaI-, CuBr-, and CuI-based devices, respectively, compare to the 14.0% value for the pristine perovskite solar cell.

Figure 1. Mesoscopic perovskite solar cell architecture.

SEM cross-sectional micrograph of a complete device with the following structure: FTO/compact- TiO_2 /mesoporous- TiO_2 / $\text{CH}_3\text{NH}_3\text{PbI}_3$ /Spiro-OMeTAD/Au.

Figure 2. Morphological analysis of lead iodide and perovskite structures.

Top-view SEM images of PbI_2 (left side) and $\text{CH}_3\text{NH}_3\text{PbI}_3$ (right side) structures: (a) pristine, (b) CuBr-, (c) CuI-, (d) NaI-, and (e) AgI-based perovskite samples deposited on a mesoporous TiO_2 -

coated FTO. This figure has been reproduced from Reference 18.

Figure 3. Effect of monovalent cation halide additives on perovskite crystallinity.

X-ray diffraction spectra of pristine and additive-based $\text{CH}_3\text{NH}_3\text{PbI}_3$ perovskite that is grown on mesoporous TiO_2 film, which is deposited on the FTO-coated glass. This figure has been reproduced from Reference 18.

Figure 4. Trace of monovalent cations in the $\text{CH}_3\text{NH}_3\text{PbI}_3$ perovskite structure.

XPS analysis of pristine, CuBr-, CuI-, NaI-, and AgI-based perovskite films. This figure has been reproduced from Reference 18.

Figure 5. Optical properties of perovskite films.

(a) The absorption spectra of perovskite films derived from pristine and additive-based lead sources measured using the PDS technique. The inset shows the corresponding Urbach energies for all samples. The error bar is defined by the SD in fitting the Urbach tail. (b) Comparison of the PDS absorption spectra of pristine and CuBr-based lead iodide and perovskite films, as well as CuBr deposited on ms- TiO_2 and CuBr-only films. This figure has been reproduced from Reference 18.

Figure 6. Effect of monovalent cation additives on the surface potential of perovskite films.

CPD line profiles recorded from pristine and additive-based perovskite films using KPFM. The AFM topography image is shown on the top. This figure has been reproduced from Reference 18.

Figure 7. Charge transport characteristics of perovskite films.

(a) J-V characteristics of hole-only devices (ITO/PEDOT:PSS/Perovskite/Au), utilized for estimating the SCLC hole mobility. Note that the current density (J) is scaled with the thickness of the perovskite layers. (b) The trends in the J_{sc} , μ_h , and μ_e for pristine and additive-based perovskite. This figure has been reproduced from Reference 18.

Figure 8. Photovoltaic performance characteristics.

(a) Current-voltage characteristics of devices under an illumination of 100 mW/cm^2 , obtained using different types of monovalent cation halides added to the lead source solution. (b) Incident photon-to-current efficiency (IPCE) spectra as a function of the wavelength of monochromatic light for the pristine, CuBr-, CuI-, NaI-, and AgI-based perovskite solar cells. This figure has been reproduced from Reference 18.

Table 1. Photovoltaic and charge transport parameters of PSC.

Summary of the photovoltaic parameters derived from J-V measurements and charge mobilities, along with the activation energy for the pristine and additive-based perovskite solar cells that show the best performance and were fabricated using the two-step deposition method. It is notable that the statistics of the photovoltaic parameters follow the same trend as the best performing devices. This table has been reproduced from Reference 18.

DISCUSSION:

A typical architecture of mesoscopic perovskite solar cells was used in this work, where a series of materials were spin-coated between a conductive substrate and a thermally-evaporated metal contact (Figure 1). The mesoporous TiO_2 layers were treated with TiCl_4 , which is reported to passivate the surface traps and to improve the interface between the electron transport layer and the absorber material^{21,22}. The perovskite layer was then deposited using a sequential two-step deposition technique. The full conversion of lead halide into perovskite in the second step is essential to achieve the highest light absorption^{16,17}, and we showed that the monovalent cation halide additives (*e.g.*, NaI and CuBr) result in a complete conversion. Furthermore, the complete coverage of the mesoporous titania layer with the perovskite over-layer is vital to eliminate potential recombination between the hole transport layer (*e.g.*, Spiro OMETAD) and the electron transport layer (*e.g.*, mesoporous TiO_2)²³. We illustrated that adding the monovalent cation halides (*e.g.*, CuI and AgI) can improve the surface coverage of the perovskite capping layer, which leads to a higher open circuit voltage for the device.

The main advantage of our method is the doping step, where we incorporated monovalent cations into the $\text{CH}_3\text{NH}_3\text{PbI}_3$ structure to improve the density of charges, the charge transport, and the conductivity of the absorber layer. As stated in the previous section, the aforementioned dopants significantly enhanced both the electron and the hole mobilities. In addition, a remarkable decrease in the charge transport activation energy, as well as in the energetic disorder of the perovskite film, was achieved by monovalent cation doping.

In this work, we have demonstrated a method to dope $\text{CH}_3\text{NH}_3\text{PbI}_3$ as an absorber layer in the mesoscopic perovskite solar cell structure. Monovalent cation halides were used to tune the morphological, optical, and electrical properties of $\text{CH}_3\text{NH}_3\text{PbI}_3$ perovskite film in order to enhance the photovoltaic performance. Therefore, we incorporated three different monovalent cations (*i.e.*, Na^+ , Cu^+ , and Ag^+), which have similar ionic radii to Pb^{2+} , in the lead source in the sequential two-step deposition of $\text{CH}_3\text{NH}_3\text{PbI}_3$. As a result, a remarkable improvement in the structural and optoelectronic properties of $\text{CH}_3\text{NH}_3\text{PbI}_3$ occurred in the presence of these additives, leading to higher PCEs for the fabricated solar cells. Therefore, our work highlights a facile way of doping the $\text{CH}_3\text{NH}_3\text{PbI}_3$ as an absorber layer, which can be used in all other configurations of perovskite solar cells (*e.g.*, planar architecture) in order to further improve the electronic quality of perovskite thin films.

The data underlying this paper are available at:

<https://www.repository.cam.ac.uk/handle/1810/260187>.

ACKNOWLEDGMENTS:

M. Abdi-Jalebi thanks Nava Technology Limited for a PhD scholarship. M.I. Dar and M. Grätzel thank the King Abdulaziz City for Science and Technology (KACST) and the Swiss National Science Foundation (SNSF) for financial support. The authors would like to thank Dr. Pierre

Mettraux in the Molecular and Hybrid Materials Characterization Center, EPFL for carrying out the XPS measurements. A. Sadhanala gratefully acknowledges financial support from the Indo-UK APEX project. S.P. Senanayak acknowledges the Royal Society London for the Newton Fellowship. R.H. Friend, M. Abdi-Jalebi, and A. Sadhanala would like to acknowledge the support from the EPSRC.

DISCLOSURES:

The authors declare that they have no competing financial interests.

REFERENCES:

1. Polman, A., Knight, M., Garnett, E. C., Ehrler, B. & Sinke, W. C. Photovoltaic materials – present efficiencies and future challenges. *Science* **352**, 307, doi:10.1126/science.aad4424 (2016).
2. Green, M. A., Ho-Baillie, A. & Snaith, H. J. The emergence of perovskite solar cells. *Nat. Photonics* **8** (7), 506–514, doi:10.1038/nphoton.2014.134 (2014).
3. Stranks, S. D. & Snaith, H. J. Metal-halide perovskites for photovoltaic and light-emitting devices. *Nat. Nanotechnol.* **10** (5), 391–402, doi:10.1038/nnano.2015.90 (2015).
4. Snaith, H. H. J. Perovskites: The Emergence of a New Era for Low-Cost, High-Efficiency Solar Cells. *The J. Phys. Chem. Lett.* **4** (21), 3623–3630, doi:10.1021/jz4020162 (2013).
5. Kojima, A., Teshima, K., Shirai, Y. & Miyasaka, T. Organometal halide perovskites as visible-light sensitizers for photovoltaic cells. *J. Am. Chem. Soc.* **131** (17), 6050–1, doi:10.1021/ja809598r (2009).
6. Kim, H.-S., *et al.* Lead iodide perovskite sensitized all-solid-state submicron thin film mesoscopic solar cell with efficiency exceeding 9%. *Sci. rep.* **2**, 591, doi:10.1038/srep00591 (2012).
7. Jeon, N. J., *et al.* Compositional engineering of perovskite materials for high-performance solar cells. *Nature* **517** (7535), 476–480, doi:10.1038/nature14133 (2014).
8. Li, X., *et al.* A vacuum flash-assisted solution process for high-efficiency large-area perovskite solar cells. *Science* **353** (6294), 58–62, doi:10.1126/science.aaf8060 (2016).
9. Manser, J. S. & Kamat, P. V Band filling with free charge carriers in organometal halide perovskites. *Nat. Photonics* **8** (9), 737–743, doi:10.1038/nphoton.2014.171 (2014).
10. Xing, G., *et al.* Long-Range Balanced Electron- and Hole-Transport Lengths in Organic-Inorganic CH₃NH₃PbI₃. *Science* **342** (6156), 344–347, doi:10.1126/science.1243167 (2013).
11. Stranks, S. D., *et al.* Electron-Hole Diffusion Lengths Exceeding 1 Micrometer in an Organometal Trihalide Perovskite Absorber. *Science* **342** (6156), 341–344, doi:10.1126/science.1243982 (2013).
12. Pazos-Outon, L. M., *et al.* Photon recycling in lead iodide perovskite solar cells. *Science* **351** (6280), 1430–1433, doi:10.1126/science.aaf1168 (2016).
13. Saliba, M., *et al.* Cesium-containing Triple Cation Perovskite Solar Cells: Improved Stability, Reproducibility and High Efficiency. *Energy Environ. Sci.* **9** (6), doi:10.1039/C5EE03874J (2016).
14. Pellet, N., *et al.* Mixed-organic-cation perovskite photovoltaics for enhanced solar-light harvesting. *Angew. Chemie - Int. Ed.* **53** (12), 3151–3157, doi:10.1002/anie.201309361

- (2014).
15. Hao, F., Stoumpos, C. C., Chang, R. P. H. & Kanatzidis, M. G. Anomalous band gap behavior in mixed Sn and Pb perovskites enables broadening of absorption spectrum in solar cells. *J. Am. Chem. Soc.* **136** (22), 8094–9, doi:10.1021/ja5033259 (2014).
 16. Dar, M. I., Abdi-Jalebi, M., Arora, N., Grätzel, M. & Nazeeruddin, M. K. Growth Engineering of CH₃NH₃PbI₃ Structures for High-Efficiency Solar Cells. *Adv. Energy Mater.* **6** (2), 1501358, doi:10.1002/aenm.201501358 (2016).
 17. Ibrahim Dar, M., *et al.* Understanding the Impact of Bromide on the Photovoltaic Performance of CH₃NH₃PbI₃ Solar Cells. *Adv. Mater.* **27** (44), 7221–7228, doi:10.1002/adma.201503124 (2015).
 18. Abdi-Jalebi, M., *et al.* Impact of Monovalent Cation Halide Additives on the Structural and Optoelectronic Properties of CH₃NH₃PbI₃ Perovskite. *Adv. Energy Mater.* **6** (10), 1502472, doi:10.1002/aenm.201502472 (2016).
 19. Yin, W.-J., Shi, T. & Yan, Y. Unusual defect physics in CH₃NH₃PbI₃ perovskite solar cell absorber. *Appl. Phys. Lett.* **104** (6), 063903/1–063903/4, doi:10.1063/1.4864778 (2014).
 20. Agiorgousis, M. L., Sun, Y.-Y., Zeng, H. & Zhang, S. Strong Covalency-Induced Recombination Centers in Perovskite Solar Cell Material CH₃NH₃PbI₃. *J. Am. Chem. Soc.* **136** (41), 14570–14575, doi:10.1021/ja5079305 (2014).
 21. Andaji Garmaroudi, Z., Abdi-Jalebi, M. & Mohammadi, M.-R. A facile low temperature route to deposit TiO₂ scattering layer for efficient dye-sensitized solar cells. *RSC Adv.* , doi:10.1039/C6RA13273A (2016).
 22. Abdi-Jalebi, M., Mohammadi, M. R. & Fray, D. J. Double-Layer TiO₂ Electrodes with Controlled Phase Composition and Morphology for Efficient Light Management in Dye-Sensitized Solar Cells. *J. of Clust. Sci.* **25** (4), 1029–1045, doi:10.1007/s10876-014-0687-3 (2014).
 23. Abdi-Jalebi, M., *et al.* Impact of a Mesoporous Titania–Perovskite Interface on the Performance of Hybrid Organic–Inorganic Perovskite Solar Cells. *The J. Phys. Chem. Lett.* **7** (16), 3264–3269, doi:10.1021/acs.jpcllett.6b01617 (2016).

Figure 1

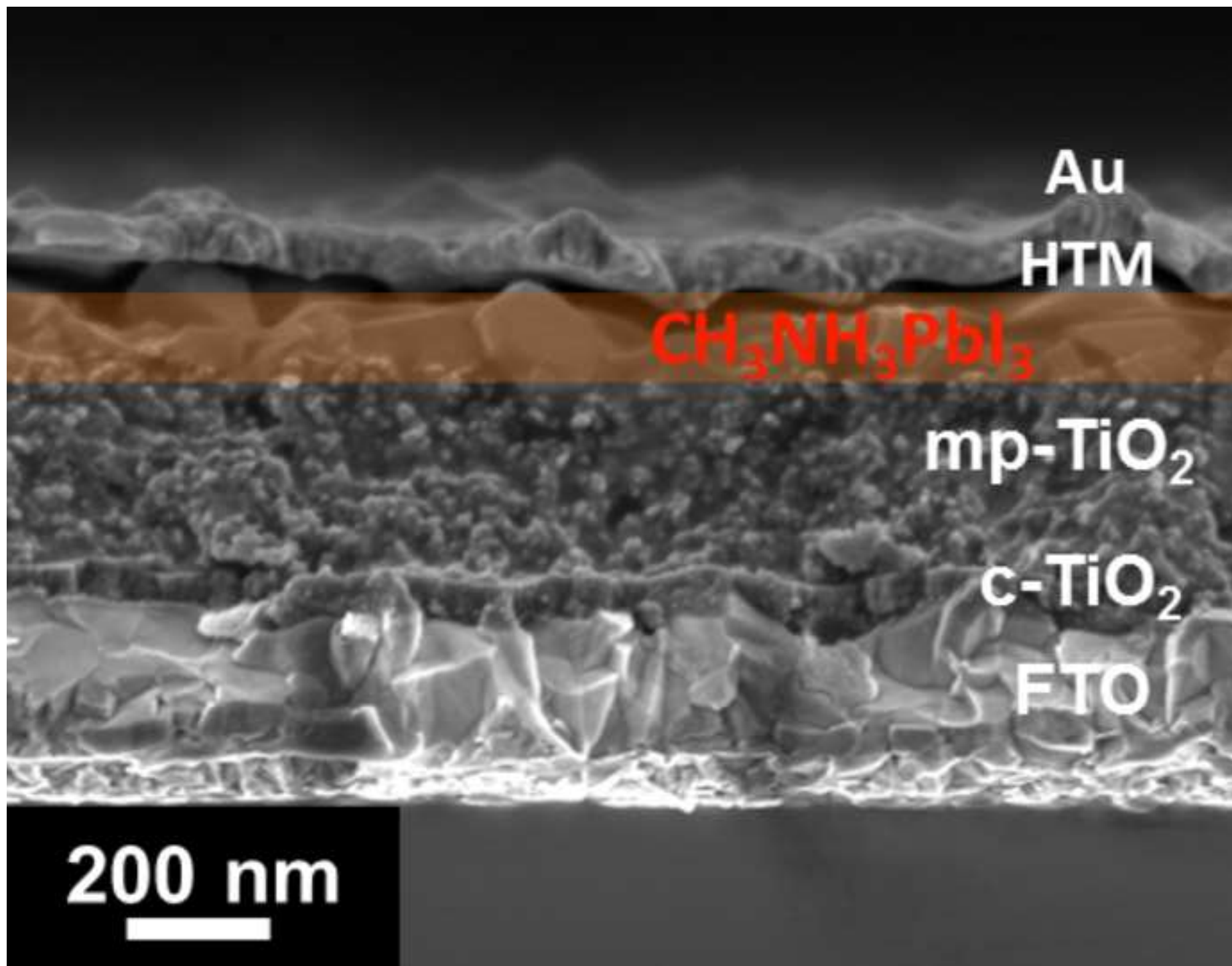


Figure 2

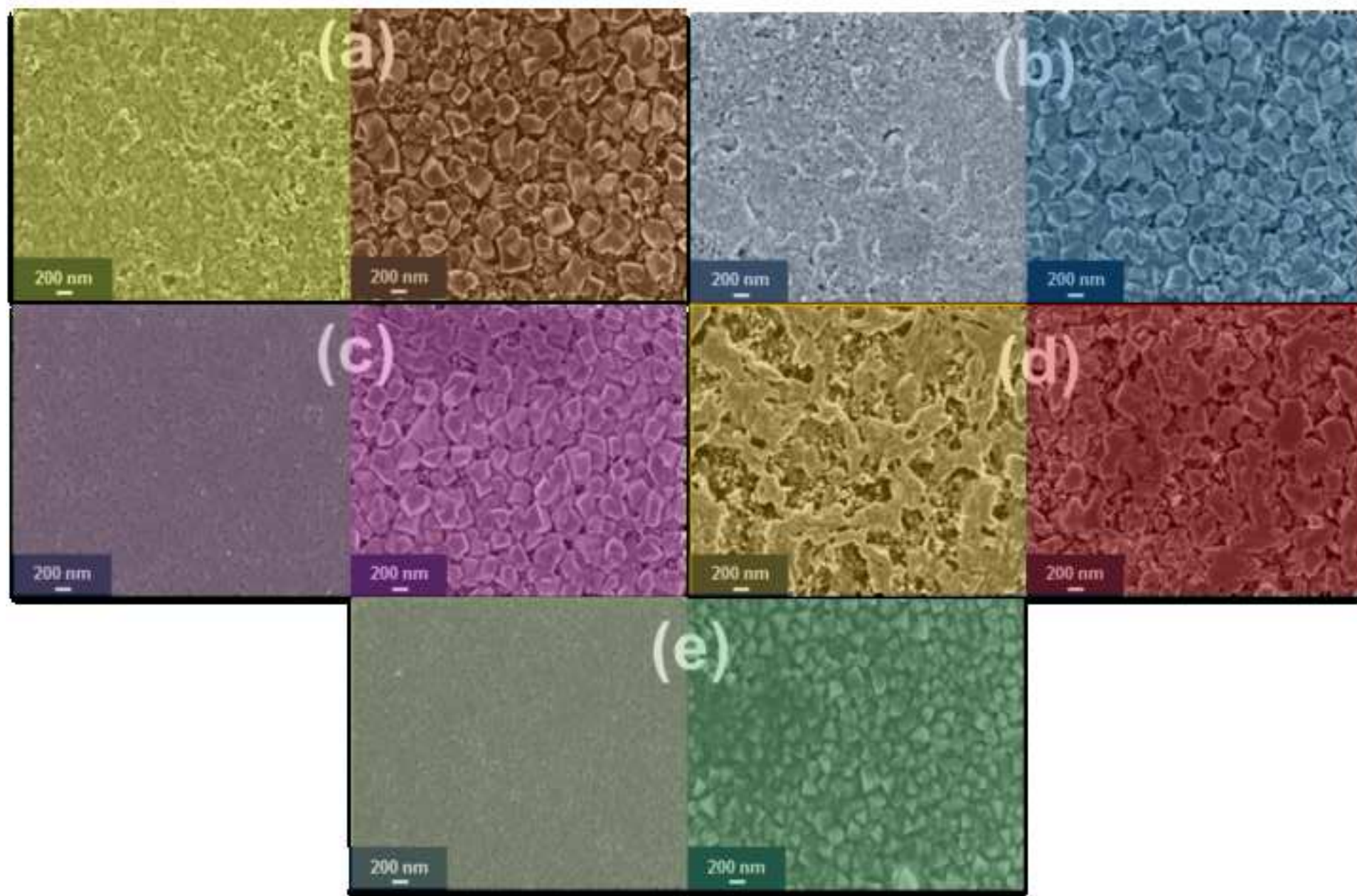


Figure 3

[Click here to download Figure Figure 3.jpg](#)

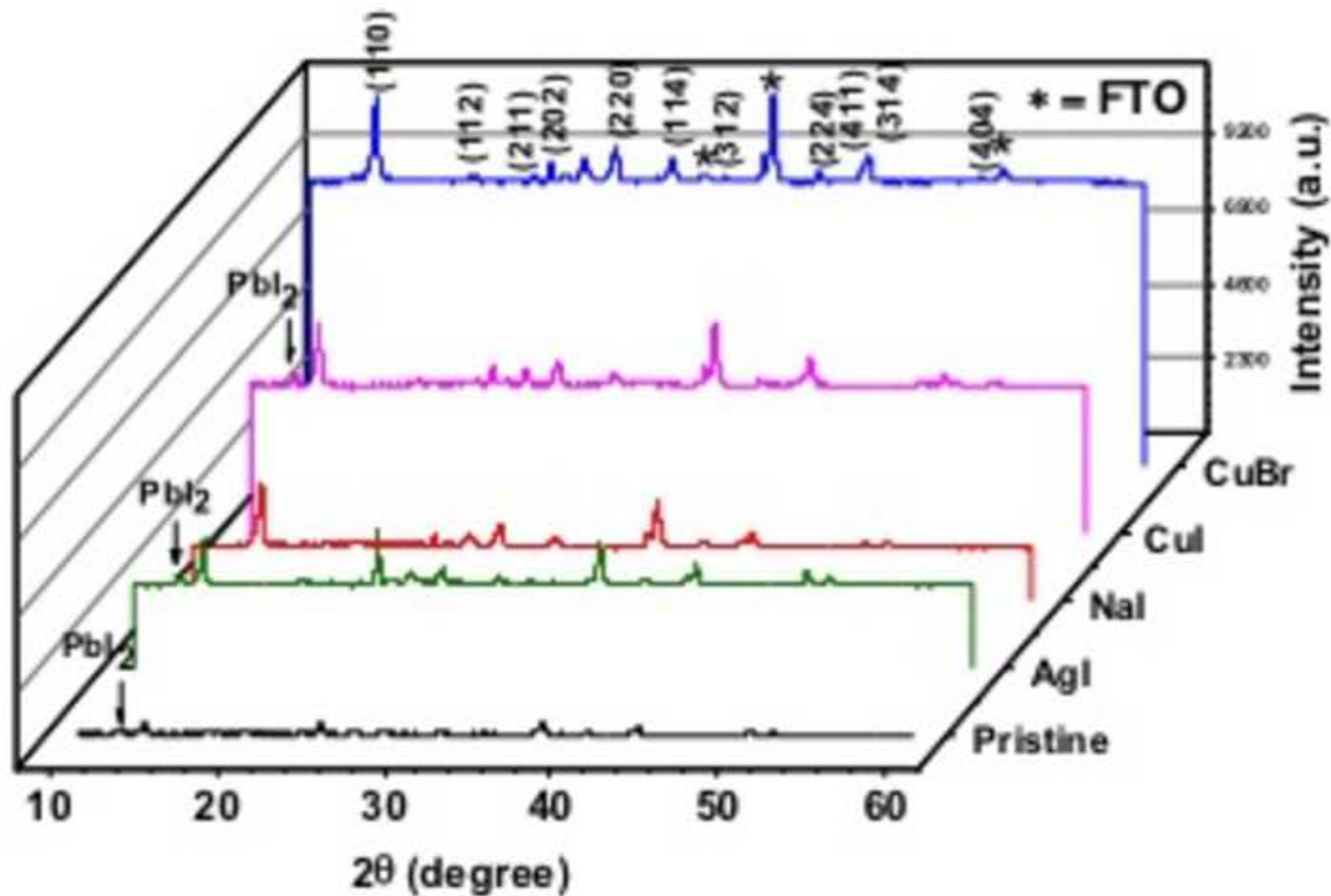


Figure 4

[Click here to download Figure Figure 4.jpg](#)

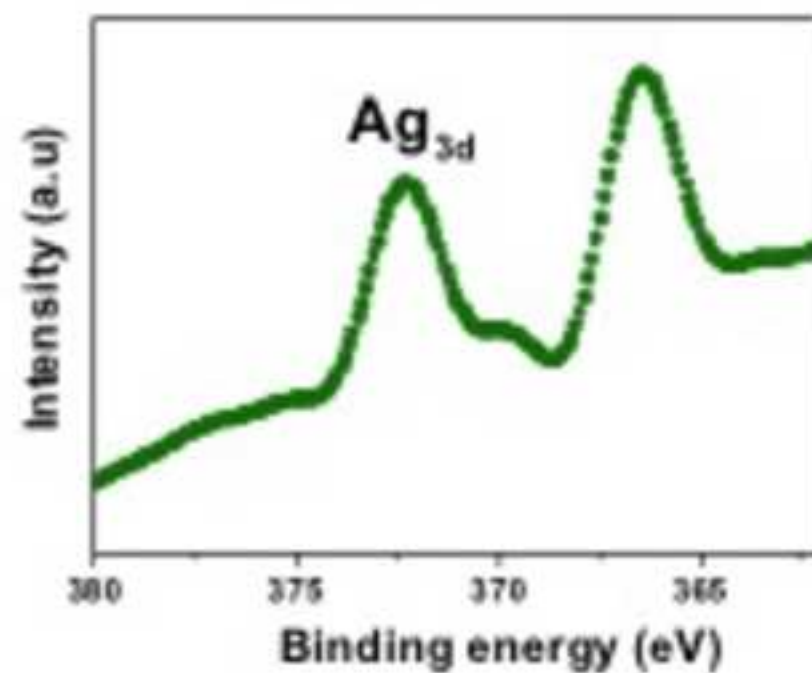
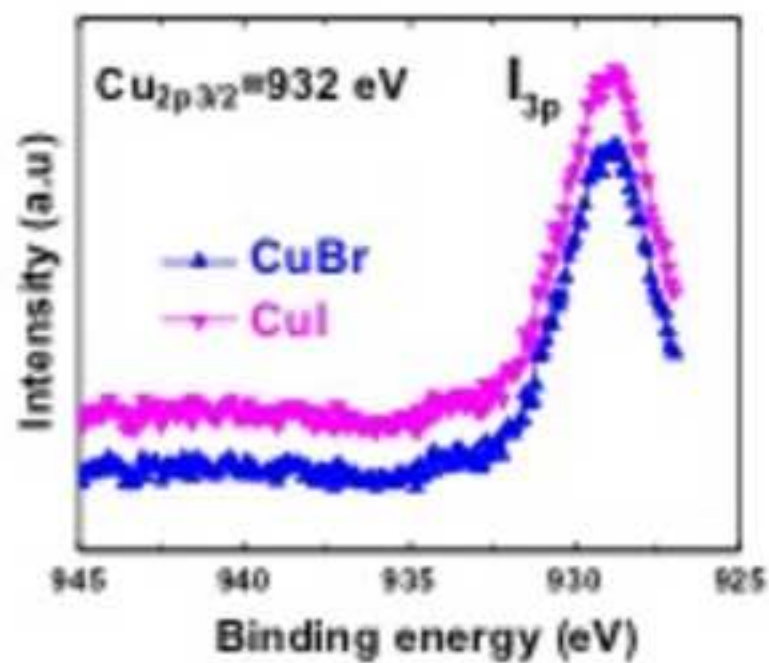
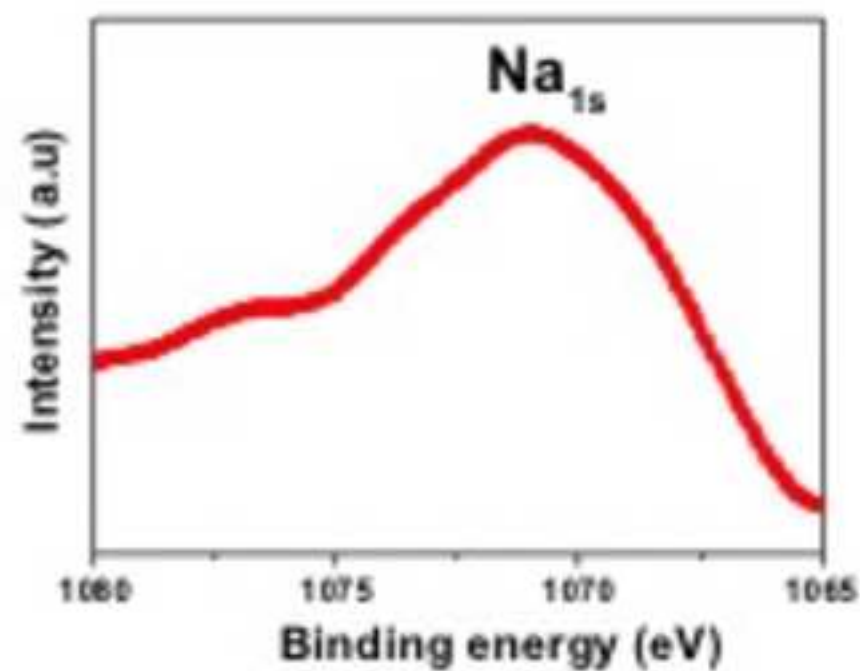
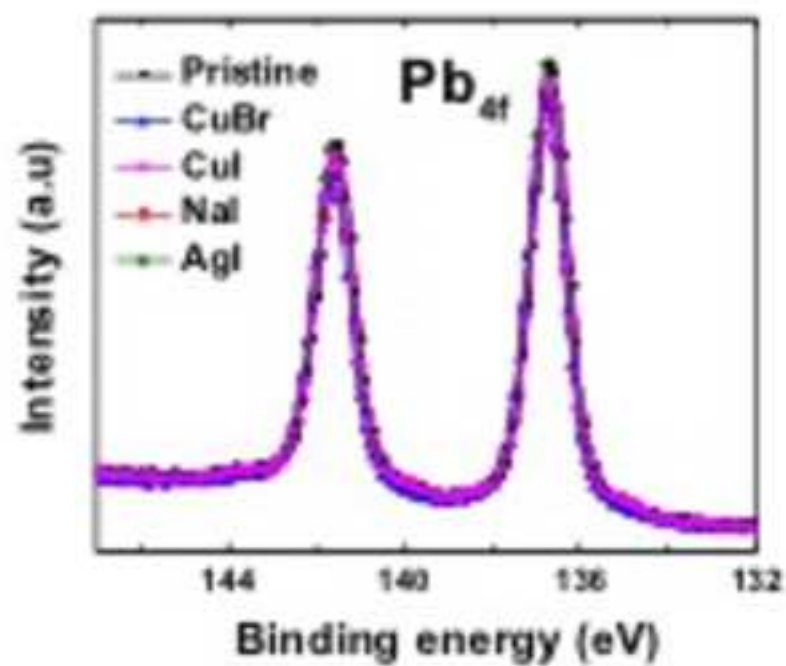


Figure 5

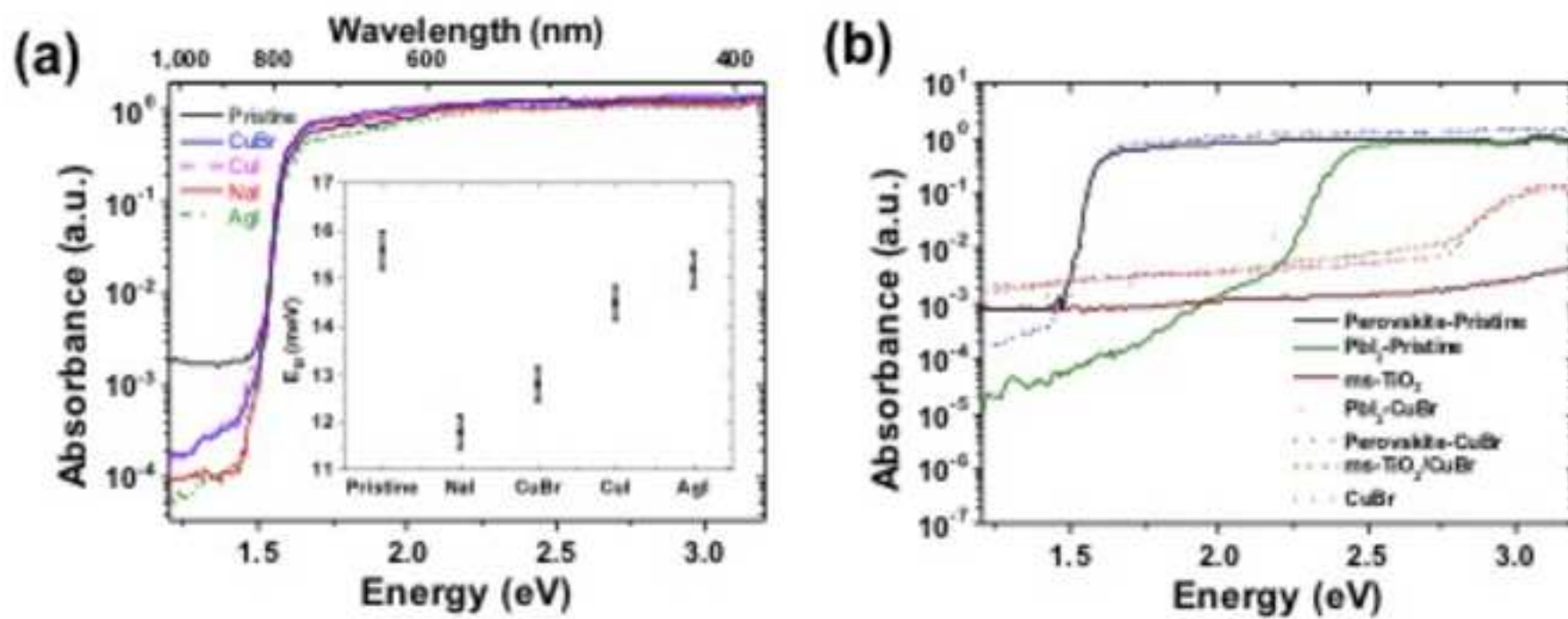
[Click here to download Figure Figure 5.jpg](#)

Figure 6

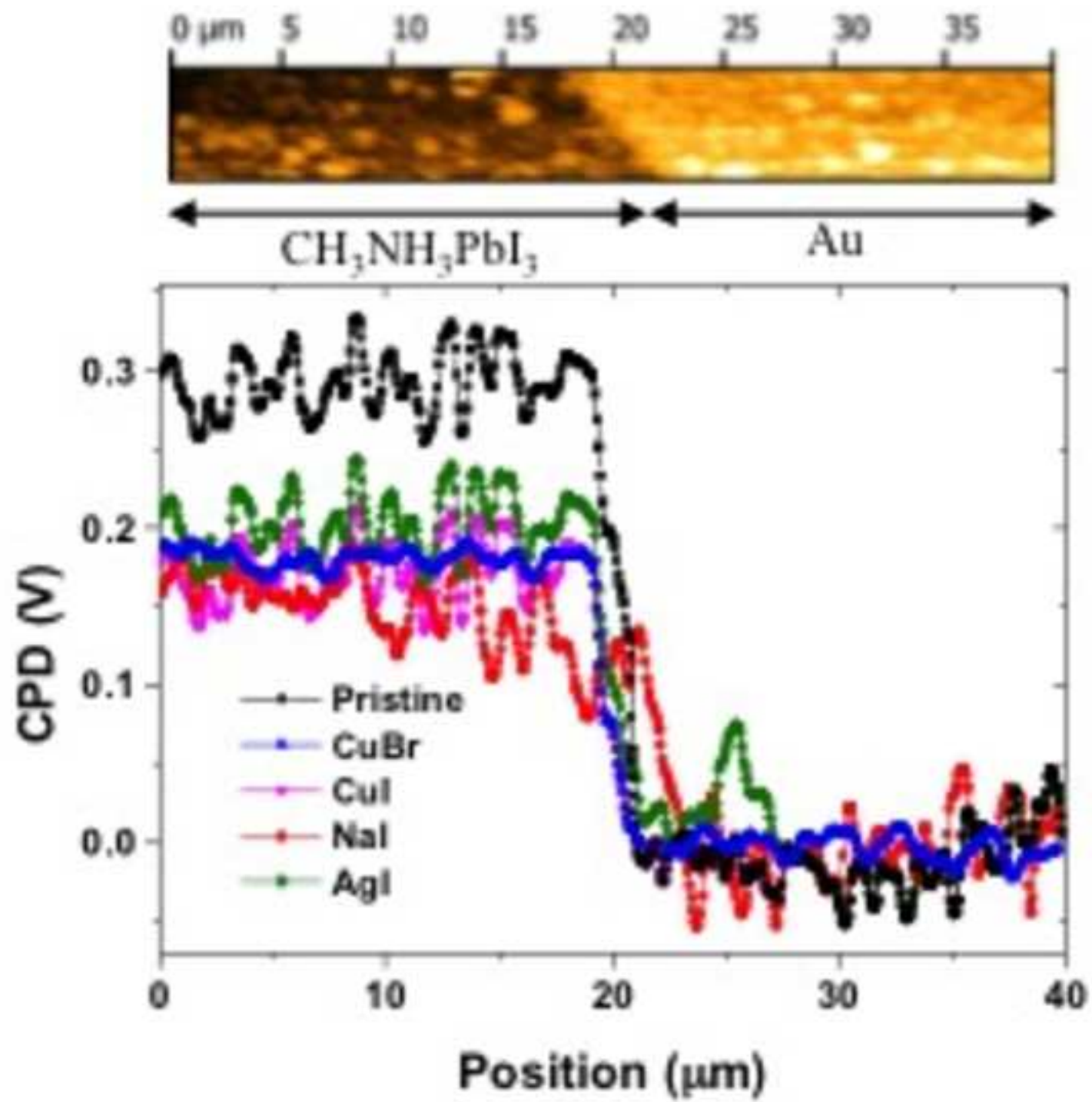


Figure 7

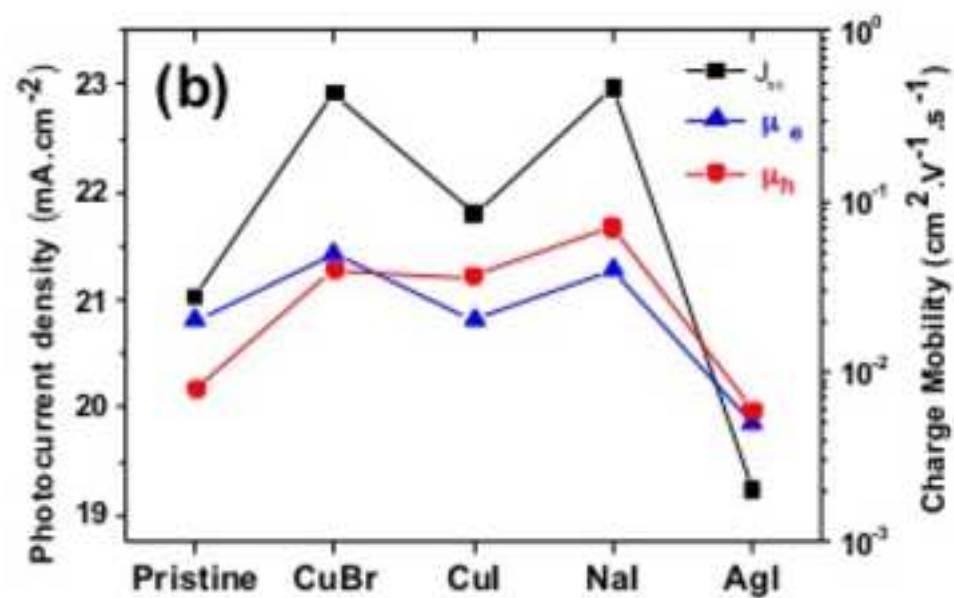
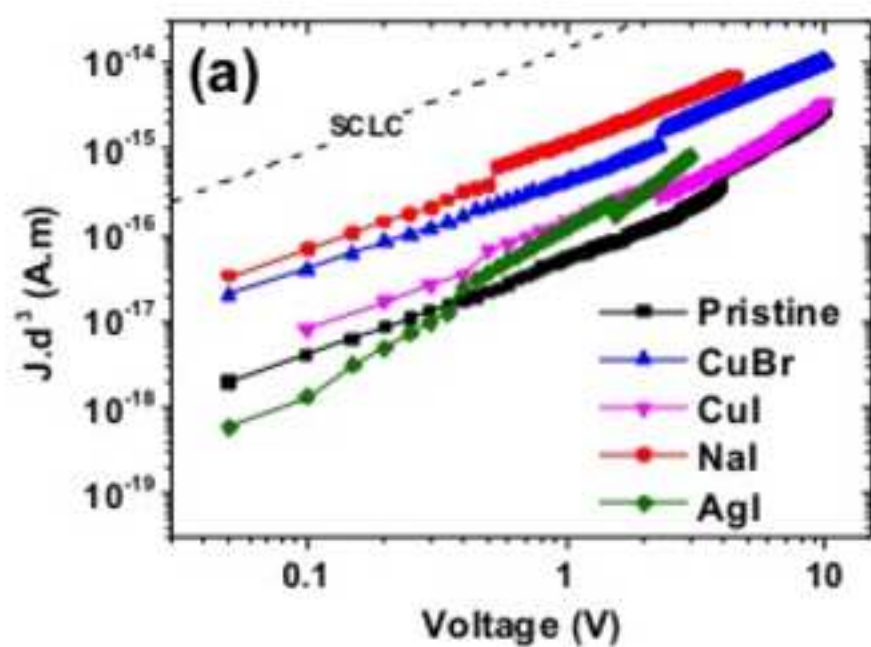
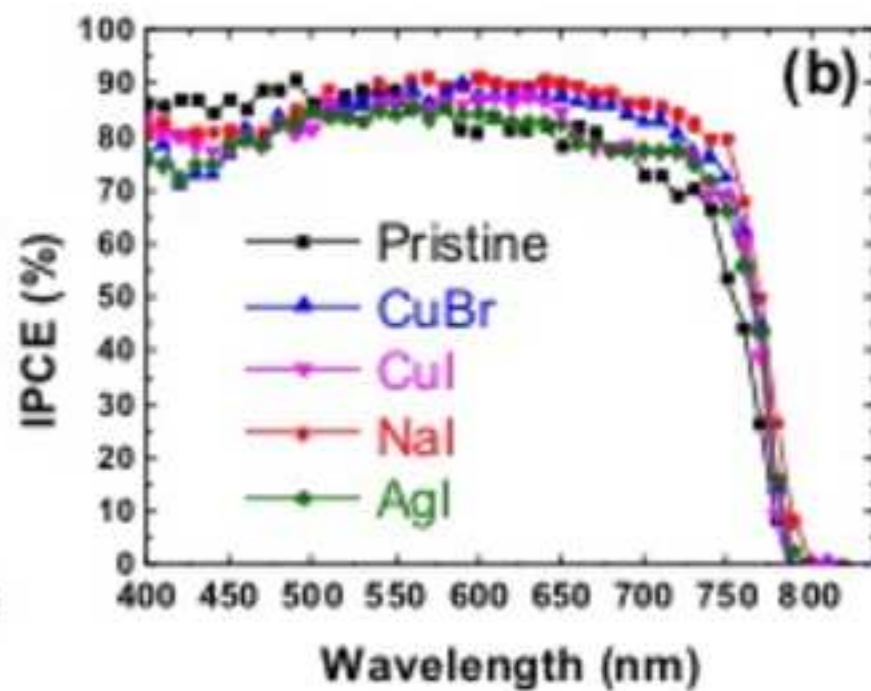
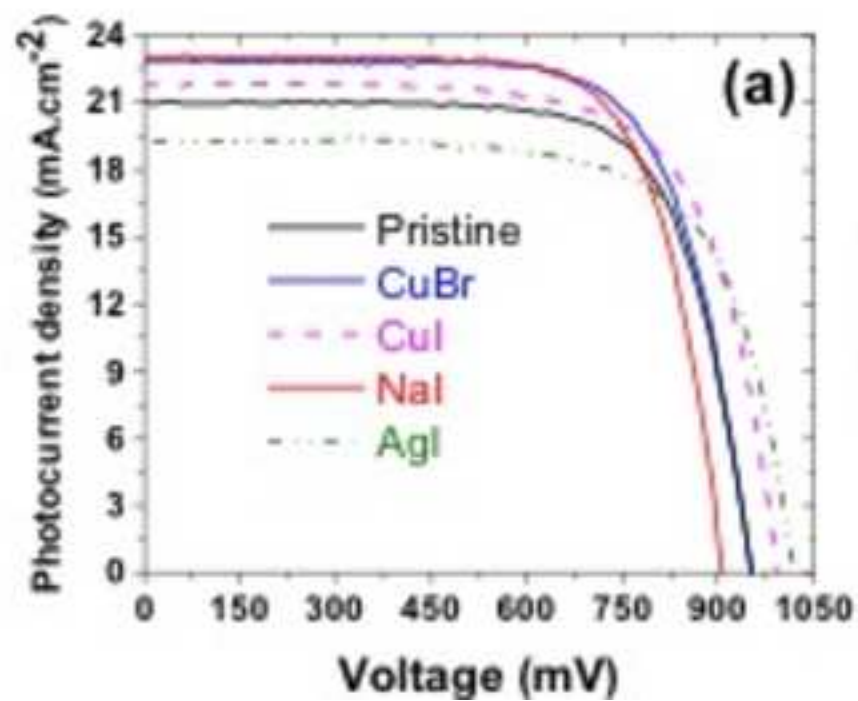
[Click here to download Figure Figure 7.jpg](#)

Figure 8

[Click here to download Figure Figure 8.jpg](#)



Type of Sample	J _{sc} (mA cm ⁻²)	V _{oc} (V)	FF	PCE (%)	m _e (cm ² /Vs)	m _h (cm ² /Vs)
Pristine	21.03	0.95	0.7	14.01	0.02	0.008
CuBr	22.92	0.95	0.72	15.61	0.05	0.04
CuI	21.81	0.99	0.71	15.25	0.02	0.036
NaI	22.97	0.9	0.73	15.14	0.04	0.07
AgI	19.24	1.02	0.72	14.18	0.005	0.006

E_A^e	E_A^h
(meV)	(meV)
135	198
88	132
94	157
77	137
105	177

Name of Material/ Equipment	Company	Catalog Number	Comments/Description
Fluorine doped Tin Oxide (FTO)-coated glass	Sigma-Aldrich	735264-1EA	Resistivity≈13 Ω/sq
Zinc powder	Sigma-Aldrich	96454	Molecular Weight 65.39
Hydrochloric acid	Sigma-Aldrich	84415	≥37 wt. %
Hellmanex detergent	Sigma-Aldrich	Z805939-1EA	pkg of 1 L
Titanium diisopropoxide bis(acetylacetonate)	Sigma-Aldrich	325252	75 wt. % in isopropanol
Titania Paste	DYESOL	MS002300	30 NR-D Transparent Titania Paste
Lead (II) iodide	Sigma-Aldrich	211168	99 wt. %
N,N-Dimethylformamide	Sigma-Aldrich	437573	ACS reagent, ≥99.8%
Methylammonium iodide	DYESOL	MS101000	Powder
SpiroMeOTAD	Sigma-Aldrich	792071	99% (HPLC)
Bis(trifluoromethane)sulfonimide lithium salt	Sigma-Aldrich	544094	99.95% trace metals basis
4-tert-Butylpyridine	Sigma-Aldrich	142379	Purity: 96%
Chlorobenzene	Sigma-Aldrich	284513	anhydrous, 99.8%
2-Propanol (IPA)	Sigma-Aldrich	278475	anhydrous, 99.5%
Ethanol	Sigma-Aldrich	2860	absolute alcohol, without additive, ≥99.8%



1 Alewife Center #200
Cambridge, MA 02140
tel. 617.945.9051
www.jove.com

Title of Article: **Tuning structural and optoelectronic properties of $\text{CH}_3\text{NH}_3\text{PbI}_3$ perovskite by monovalent cation halide additives**

Author(s): **Mojtaba Abdi-Jalebi, M. Ibrahim Dar, Aditya Sadhanala, Satyaprasad P. Senanayak, Michael Grätzel, Richard H. Friend**

Item 1 (check one box): The Author elects to have the Materials be made available (as described at <http://www.jove.com/publish>) via: ☐ Standard Access ☒ Open Access

Item 2 (check one box):

- ☒ The Author is NOT a United States government employee.
- ☐ The Author is a United States government employee and the Materials were prepared in the course of his or her duties as a United States government employee.
- ☐ The Author is a United States government employee but the Materials were NOT prepared in the course of his or her duties as a United States government employee.

ARTICLE AND VIDEO LICENSE AGREEMENT

1. Defined Terms. As used in this Article and Video License Agreement, the following terms shall have the following meanings: “**Agreement**” means this Article and Video License Agreement; “**Article**” means the article specified on the last page of this Agreement, including any associated materials such as texts, figures, tables, artwork, abstracts, or summaries contained therein; “**Author**” means the author who is a signatory to this Agreement; “**Collective Work**” means a work, such as a periodical issue, anthology or encyclopedia, in which the Materials in their entirety in unmodified form, along with a number of other contributions, constituting separate and independent works in themselves, are assembled into a collective whole; “**CRC License**” means the Creative Commons Attribution 3.0 Agreement, the terms and conditions of which can be found at: <http://creativecommons.org/licenses/by/3.0/us/legalcode>; “**Derivative Work**” means a work based upon the Materials or upon the Materials and other pre-existing works, such as a translation, musical arrangement, dramatization, fictionalization, motion picture version, sound recording, art reproduction, abridgment, condensation, or any other form in which the Materials may be recast, transformed, or adapted; “**Institution**” means the institution, listed on the last page of this Agreement, by which the Author was employed at the time of the creation of the Materials; “**JoVE**” means MyJoVE Corporation, a Massachusetts corporation and the publisher of *The Journal of Visualized Experiments*;

“**Materials**” means the Article and / or the Video; “**Parties**” means the Author and JoVE; “**Video**” means

any video(s) made by the Author, alone or in conjunction with any other parties, or by JoVE or its affiliates or agents, individually or in collaboration with the Author or any other parties, incorporating all or any portion of the Article, and in which the Author may or may not appear.

2. Background. The Author, who is the author of the Article, in order to ensure the dissemination and protection of the Article, desires to have the JoVE publish the Article and create and transmit videos based on the Article. In furtherance of such goals, the Parties desire to memorialize in this Agreement the respective rights of each Party in and to the Article and the Video.

3. Grant of Rights in Article. In consideration of JoVE agreeing to publish the Article, the Author hereby grants to JoVE, subject to **Sections 4 and 7** below, the exclusive, royalty-free, perpetual (for the full term of copyright in the Article, including any extensions thereto) license (a) to publish, reproduce, distribute, display and store the Article in all forms, formats and media whether now known or hereafter developed (including without limitation in print, digital and electronic form) throughout the world, (b) to translate the Article into other languages, create adaptations, summaries or extracts of the Article or other Derivative Works (including, without limitation, the Video) or Collective Works based on all or any portion of the Article and exercise all of the rights set forth in (a) above in such translations, adaptations, summaries, extracts, Derivative Works or Collective Works and (c) to license others to do any or all of the above. The foregoing rights may be exercised in all media and formats,

set forth in, the CRC License.

4. Retention of Rights in Article. Notwithstanding the exclusive license granted to JoVE in **Section 3** above, the Author shall, with respect to the Article, retain the non-exclusive right to use all or part of the Article for the non-commercial purpose of giving lectures, presentations or teaching classes, and to post a copy of the Article on the Institution's website or the Author's personal website, in each case provided that a link to the Article on the JoVE website is provided and notice of JoVE's copyright in the Article is included. All non-copyright intellectual property rights in and to the Article, such as patent rights, shall remain with the Author.

5. Grant of Rights in Video – Standard Access. This **Section 5** applies if the "Standard Access" box has been checked in **Item 1** above or if no box has been checked in **Item 1** above. In consideration of JoVE agreeing to produce, display or otherwise assist with the Video, the Author hereby acknowledges and agrees that, Subject to **Section 7** below, JoVE is and shall be the sole and exclusive owner of all rights of any nature, including, without limitation, all copyrights, in and to the Video. To the extent that, by law, the Author is deemed, now or at any time in the future, to have any rights of any nature in or to the Video, the Author hereby disclaims all such rights and transfers all such rights to JoVE.

6. Grant of Rights in Video – Open Access. This **Section 6** applies only if the "Open Access" box has been checked in **Item 1** above. In consideration of JoVE agreeing to produce, display or otherwise assist with the Video, the Author hereby grants to JoVE, subject to **Section 7** below, the exclusive, royalty-free, perpetual (for the full term of copyright in the Article, including any extensions thereto) license (a) to publish, reproduce, distribute, display and store the Video in all forms, formats and media whether now known or hereafter developed (including without limitation in print, digital and electronic form) throughout the world, (b) to translate the Video into other languages, create adaptations, summaries or extracts of the Video or other Derivative Works or Collective Works based on all or any portion of the Video and exercise all of the rights set forth in (a) above in such translations, adaptations, summaries, extracts, Derivative Works or Collective Works and (c) to license others to do any or all of the above. The foregoing rights may be exercised in all media and formats, whether now known or hereafter devised, and include the right to make such modifications as are technically necessary to exercise the rights in other media and formats.

7. Government Employees. If the Author is a United States government employee and the Article was prepared in the course of his or her duties as a United States government employee, as indicated in **Item 2** above, and any of the licenses or grants granted by the Author hereunder exceed the scope of the 17 U.S.C. 403, then the rights granted hereunder shall be limited to the

maximum rights permitted under such statute. In such case, all provisions contained herein that are not in conflict with such statute shall remain in full force and effect, and all provisions contained herein that do so conflict shall be deemed to be amended so as to provide to JoVE the maximum rights permissible within such statute.

8. Likeness, Privacy, Personality. The Author hereby grants JoVE the right to use the Author's name, voice, likeness, picture, photograph, image, biography and performance in any way, commercial or otherwise, in connection with the Materials and the sale, promotion and distribution thereof. The Author hereby waives any and all rights he or she may have, relating to his or her appearance in the Video or otherwise relating to the Materials, under all applicable privacy, likeness, personality or similar laws.

9. Author Warranties. The Author represents and warrants that the Article is original, that it has not been published, that the copyright interest is owned by the Author (or, if more than one author is listed at the beginning of this Agreement, by such authors collectively) and has not been assigned, licensed, or otherwise transferred to any other party. The Author represents and warrants that the author(s) listed at the top of this Agreement are the only authors of the Materials. If more than one author is listed at the top of this Agreement and if any such author has not entered into a separate Article and Video License Agreement with JoVE relating to the Materials, the Author represents and warrants that the Author has been authorized by each of the other such authors to execute this Agreement on his or her behalf and to bind him or her with respect to the terms of this Agreement as if each of them had been a party hereto as an Author. The Author warrants that the use, reproduction, distribution, public or private performance or display, and/or modification of all or any portion of the Materials does not and will not violate, infringe and/or misappropriate the patent, trademark, intellectual property or other rights of any third party. The Author represents and warrants that it has and will continue to comply with all government, institutional and other regulations, including, without limitation all institutional, laboratory, hospital, ethical, human and animal treatment, privacy, and all other rules, regulations, laws, procedures or guidelines, applicable to the Materials, and that all research involving human and animal subjects has been approved by the Author's relevant institutional review board.

10. JoVE Discretion. If the Author requests the assistance of JoVE in producing the Video in the Author's facility, the Author shall ensure that the presence of JoVE employees, agents or independent contractors is in accordance with the relevant regulations of the Author's institution. If more than one author is listed at the beginning of this Agreement, JoVE may, in its sole discretion, elect not take any action with respect to the Article until such time as it has received complete, executed Article and Video License Agreements from each such author. JoVE reserves the right, in its absolute and sole discretion and without giving any reason therefore, to

ARTICLE AND VIDEO LICENSE AGREEMENT- UK

accept or decline any work submitted to JoVE. JoVE and its employees, agents and independent contractors shall have full, unfettered access to the facilities of the Author or of the Author's institution as necessary to make the Video, whether actually published or not. JoVE has sole discretion as to the method of making and publishing the Materials, including, without limitation, to all decisions regarding editing, lighting, filming, timing of publication, if any, length, quality, content and the like.

11. Indemnification. The Author agrees to indemnify JoVE and/or its successors and assigns from and against any and all claims, costs, and expenses, including attorney's fees, arising out of any breach of any warranty or other representations contained herein. The Author further agrees to indemnify and hold harmless JoVE from and against any and all claims, costs, and expenses, including attorney's fees, resulting from the breach by the Author of any representation or warranty contained herein or from allegations or instances of violation of intellectual property rights, damage to the Author's or the Author's institution's facilities, fraud, libel, defamation, research, equipment, experiments, property damage, personal injury, violations of institutional, laboratory, hospital, ethical, human and animal treatment, privacy or other rules, regulations, laws, procedures or guidelines, liabilities and other losses or damages related in any way to the submission of work to JoVE, making of videos by JoVE, or publication in JoVE or elsewhere by JoVE. The Author shall be responsible for, and shall hold JoVE harmless from, damages caused by lack of sterilization, lack of cleanliness or by contamination due to the making of a video by JoVE its employees, agents or independent contractors. All sterilization, cleanliness or decontamination procedures shall be solely the responsibility

of the Author and shall be undertaken at the Author's expense. All indemnifications provided herein shall include JoVE's attorney's fees and costs related to said losses or damages. Such indemnification and holding harmless shall include such losses or damages incurred by, or in connection with, acts or omissions of JoVE, its employees, agents or independent contractors.

12. Fees. To cover the cost incurred for publication, JoVE must receive payment before production and publication the Materials. Payment is due in 21 days of invoice. Should the Materials not be published due to an editorial or production decision, these funds will be returned to the Author. Withdrawal by the Author of any submitted Materials after final peer review approval will result in a US\$1,200 fee to cover pre-production expenses incurred by JoVE. If payment is not received by the completion of filming, production and publication of the Materials will be suspended until payment is received.

13. Transfer, Governing Law. This Agreement may be assigned by JoVE and shall inure to the benefits of any of JoVE's successors and assignees. This Agreement shall be governed and construed by the internal laws of the Commonwealth of Massachusetts without giving effect to any conflict of law provision thereunder. This Agreement may be executed in counterparts, each of which shall be deemed an original, but all of which together shall be deemed to be one and the same agreement. A signed copy of this Agreement delivered by facsimile, e-mail or other means of electronic transmission shall be deemed to have the same legal effect as delivery of an original signed copy of this Agreement.

A signed copy of this document must be sent with all new submissions. Only one Agreement required per submission.

CORRESPONDING AUTHOR:

Name:

MOJTABA ABDI-JALEBI

Department:

Physics

Institution:

University of Cambridge

Article Title:

Tuning Structural and optoelectronic properties of $\text{CH}_3\text{NH}_3\text{PbI}_3$ Perovskite by monovalent cation halide additives

Signature:

Mojtaba Abdi-Jalebi

Date:

22.07.2016

Please submit a signed and dated copy of this license by one of the following three methods:

- 1) Upload a scanned copy of the document as a pdf on the JoVE submission site;
- 2) Fax the document to +1.866.381.2236;
- 3) Mail the document to JoVE / Attn: JoVE Editorial / 1 Alewife Center #200 / Cambridge, MA 02139

For questions, please email submissions@jove.com or call +1.617.945.9051

Mojtaba Abdi-Jalebi
Research Associate in Cavendish



**UNIVERSITY OF
CAMBRIDGE**
Cavendish Laboratory

Date: 12 November 2016

Journal of Visualized Experiments (JoVE),

Dear Dr Nguyen,

We are herewith submitting our revised manuscript entitled, “**Monovalent Cation Doping of $\text{CH}_3\text{NH}_3\text{PbI}_3$ for Efficient Perovskite Solar Cells**” to be considered for publication in *Journal of Visualized Experiments*. We consider the work to be of immense interest to the readers of *Journal of Visualized Experiments* for the following reasons.

We are providing below a detailed, point-by-point response to the questions raised by the Reviewers. We are grateful for the comments made by the Reviewers, which resulted in important additions to our work. We hope that our revised manuscript that addresses all the reviews concerns would be considered for publication in *Journal of Visualized Experiments* to which we look forward.

Thank you very much for your consideration.

Yours sincerely,

Mojtaba Abdi-Jalebi

Cavendish Laboratory
JJ Thompson Avenue
Cambridge, CB3 0HE

Telephone: +44 1223 337218
Fax: +44 1223 764515
E-mail: ma571@cam.ac.uk
Web: www.oe.phy.cam.ac.uk

Editorial comments:

The manuscript has been modified by the Science Editor to comply with the JoVE formatting standard. Please maintain the current formatting throughout the manuscript. The updated manuscript (55307_R1_083116.docx) is located in your Editorial Manager account. In the revised PDF submission, there is a hyperlink for downloading the .docx file. Please download the .docx file and use this updated version for any future revisions.

1. Please abbreviate journal titles.

It is corrected now.

2. There are a few grammar issues to be corrected:

-2.1.1.1. "Cover the active area of the FTO glass with scotch type" assuming you meant scotch tape, but this is also branding, so you should change this to simply tape, clear tape, or sticky tape.

It is corrected now.

-2.1.1.5. "Wash the FTO with water and remove the tapes." Tape.

It is corrected now.

3. Additional detail is required in step 2.1.3: "Dissolve 2 M of hydrochloric acid (HCl) in distilled water" how much water, for what final volume?

M means moles.Liter⁻¹. M is now replaced by moles.Liter⁻¹ which shows the concentration of HCl in distilled water.

4. Unnecessary branding should be removed: Scotch tape.

Scotch tape is now eliminated from the manuscript.

Reviewers' comments:

Reviewer #1:

Manuscript Summary:

The manuscript reports doping of various cations to improve the performance of MAPI based devices, with new insights on how the dopants improves various optoelectronic properties of the MAPI. Significant part of the manuscript have been reproduced from reference number 18 (Advanced energy material). The work can be published after a major revision, which are as following:

1) Why the dopants are improving the properties are not fully understood? Which site they are replacing? This should be shown with other experimental tools.

As we stated in the manuscript, monovalent cation halide with similar ionic radii to Pb^{2+} , including Cu^+ , Na^+ and Ag^+ , were added to explore possibility of doping in the $\text{CH}_3\text{NH}_3\text{PbI}_3$ (Pb site). The enhancement in the properties (e.g. photovoltaic performance) is explained due to the various reasons created in the presence of these monovalent cations such as formation of uniform and continuous perovskite film, better conversion of PbI_2 into $\text{CH}_3\text{NH}_3\text{PbI}_3$, improved loading of perovskite into mesoporous scaffold as well as the enhancement in the bulk charge transport along with a minimization of electronic disorder, pointing towards possible surface passivation.

2) During doping with CuBr is there a possibility for the formation of $\text{MAPbBr}_x\text{I}_{3-x}$?

We agree with the reviewer that the Br might present in the final structure. However, since the concentration of the dopants is about 0.02 mol.L^{-1} , which is very small for Br to effect on the properties as we observed the same band-edge for CuBr based perovskite (Figure 5a).

3) Why the CPD signals are noisy?

Since the surface of perovskite layer is normally rough, the CPD signals around the perovskite region are a bit noisy as the CPD signal for AgI based perovskite which is the smoothest sample shows the least noise. In addition, in the KPFM measurement, we are interested to find out the change of CPD at the interface between the perovskite film and the gold contact which is a representative of the change in the work function of the materials. Therefore, the signals in the perovskite region is not the main point of the data.

4) Device statistics needs to be presented to understand the improvement in various device parameters.

The JV parameters for the best performing devices are consistent with the statistics following the same trend. The statistics can be provided while for JOVE which is a method based journal, we think it is not necessary to include that in the main article. However, we add the below sentence in the manuscript to confirm this.

"It is notable that the statistics of the photovoltaic parameters follow the same trend as the best performing devices"

5) IPCE of 'MAPI' does not reflect an improvement compared to 'doped MAPI'.

We did calculate the integrated current from the IPCE curves and the resulted photocurrent density is in agreement with the J_{sc} improvement in presence of dopants extracted from the JV measurement.

6) Line number 289: "...filling the transport traps"- How the transport traps are filled? Should be discussed.

It is plausible that the presence of stable +1 oxidation states of the cations (e.g. Na^+ , Cu^+ , Ag^+) results in passivation of hole traps in the system. This is indicated from the PDS spectra as well as the KPFM measurements which indicate a modification of the HOMO levels with cationic doping.

7) What could be the role of the dopants for improvement in crystallization and surface coverage (SEM)?

As it is shown in the Figure 3, the PbI₂ peak is vanished for NaI and CuBr sample which confirms the complete conversion of PbI₂ into CH₃NH₃PbI₃ while a residue of PbI₂ can be seen for the pristine sample. In addition, the SEM images (Figure 2) shows a different morphology of perovskite and PbI₂ for the NaI sample and a full pin hole free film is formed for the AgI based perovskite. Therefore, these cations can indeed effect on the crystallization and conversion of PbI₂ into CH₃NH₃PbI₃ as well as the formation of perovskite capping layer.

Major Concerns:
N/A

Minor Concerns:
N/A

Additional Comments to Authors:
N/A

Reviewer #2:

Manuscript Summary:

In this manuscript, authors doped monovalent cation halide salts (NaI, CuBr, CuI, and AgI) into the PbI₂ precursor solution in the sequential deposition method. They studied the morphology and optoelectronic properties of the resultant perovskite films with the presence of these monovalent cations.

Major Concerns:

Although authors tried to investigate the effect of the monovalent cation additives on the perovskite layer from different aspects, some issues are not clear. For example:

1. Authors studied the effect of CuBr additive on the perovskite film. Basically, the bromine additive could affect the properties of perovskite film. The reviewer thinks that the authors had better decouple the influences of Cu⁺ and Br⁻.

We agree with the reviewer that the Br might effect in the final structure. However, since the concentration of the dopants is about 0.02 mol.L⁻¹, which is very small for Br to effect on the properties as we observed the same band-edge for CuBr based perovskite (Figure 5a) while the absorption tail in the PDS spectra for CuBr sample which is originated from the intrinsic absorption of Cu based halide (Figure 5b) confirms the influence of Cu⁺.

2. Authors claimed that, the density of charges, the charge mobility, and the conductivity of the perovskite layer were improved by monovalent cation doping. The reviewer thinks that the mobility and conductivity improvements are reasonable, but the reviewer is intrigued to know how the additives could increase the density of charges in the perovskite layer.

We believe, the presence of stable +1 oxidation states of the cations would result in passivation of hole traps in the system which can lead to a higher charge density. A clear signature of the increase in charge density is also shown from the modification of the sub-band gap levels in the PDS spectra and the shift in the HOMO level (valence band) of the perovskite upon addition of the cationic dopant.

Mojtaba Abdi-Jalebi
Research Associate in Cavendish



**UNIVERSITY OF
CAMBRIDGE**
Cavendish Laboratory

Thus, the reviewer thinks that this manuscript may need some revision before publication.

Minor Concerns:

N/A

Additional Comments to Authors:

N/A



[Click here to access/download](#)

Supplemental File (as requested by JoVE)
Permissions & Reprint.docx

